Journal of Nuclear Materials 386–388 (2009) 661–665

Contents lists available at ScienceDirect

Journal of Nuclear Materials

journal homepage: www.elsevier.com/locate/jnucmat

Precipitate evolution in low-nickel austenitic stainless steels during neutron irradiation at very low dose rates

Y. Isobe [a,*], M. Sagisaka [a], F.A. Garner [b], S. Fujita [c], T. Okita [c]

[a] *Nuclear Fuels Limited, Osaka, Japan*
[b] *Pacific Northwest National Laboratory, Richland WA, USA*
[c] *University of Tokyo, Tokyo, Japan*

A B S T R A C T

Neutron-induced microstructural evolution in response to long term irradiation at very low dose rates was studied for a Russian low-nickel austenitic stainless steel designated X18H9 that is analogous to AISI 304. The irradiated samples were obtained from an out-of-core support column for the pressure vessel of the BN-600 fast reactor with doses ranging from 1.7 to 20.5 dpa generated at 3.8×10^{-9} to 4.3×10^{-8} dpa/s. The irradiation temperatures were in a very narrow range of 370–375 °C. Microstructural observation showed that in addition to voids and dislocations, an unexpectedly high density of small G-phase precipitates was formed that are not usually observed at higher dpa rates in this temperature range. A similar behavior was observed in a Western stainless steel, namely AISI 304 stainless steel, irradiated at similar temperatures and somewhat higher dpa rates in the EBR-II fast reactor, indicating that irradiation at low dpa rates for many years can lead to a different precipitate microstructure and therefore different associated changes in matrix composition than are generated at higher dpa rates. The contribution of such radiation-induced precipitation to changes in electrical resistivity was measured in the X18H9 specimens and was shown to cause significant deviation from predictions based only on void swelling.

1. Introduction

Not all components of a fusion reactor will be subjected to high atomic displacement rates. Some components outside the plasma containment may experience relatively low displacement rates but data generated under long-term irradiation at low dpa rates are more difficult to obtain.

In the present study the neutron-induced microstructural evolution in response to long term irradiation at very low dose rates was studied for a Russian low-nickel austenitic stainless steel that is analogous to AISI 304. The irradiated samples were obtained from an out-of-core anti-crush support column for the pressure vessel of the BN-600 fast reactor. Specimens chosen for examination had doses ranging from 1.7 to 20.5 dpa generated at 3.8×10^{-9} to 4.3×10^{-8} dpa/s. The irradiation temperatures were in a very narrow range of 370–375 °C.

2. Experimental details

The pipe being examined served for almost three decades in the BN-600 fast reactor located in Zarechney, Russia. It was removed for examination in support of plant life extension efforts. This power plant reached it 30 year lifetime in 2008. The pipe was originally produced by extrusion but due to the age of this pipe no record has survived concerning it its initial post-production thermal–mechanical condition.

The pipe's measured composition after production was specified in its certificate and was found to be Fe–8.75Ni–17.66Cr–1.36Mn–0.38Si–0.21Cu–0.09C–0.025P–0.020S in wt% as shown in Table 1. The Russian designation for this steel is X18H9 and is analogous to AISI 304 stainless steel. The pipe was originally 9.5 cm in diameter with 2.0 cm thick walls. Some small changes in dimension are expected due to swelling, phase instability and possibly light corrosion. Sodium was flowing on both the inside and outside of the pipe. There was very little change in temperature axially and radially in the pipe because the pipe lay far outside the core. The primary cause of temperature increase is gamma heating at rather low levels. Across the wall thickness the temperature increase due to gamma heating was calculated to be <1 °C. Such small variations insure that the primary operational variable in this examination is that of dpa rate.

Using a diamond milling machine remotely in a hot cell, five annular sections were cut at various elevations on the pipe and their microstructure and changes in resistivity were evaluated. The irradiation conditions of each section are shown in Table 2.

* Corresponding author.
E-mail address: isobe@nfi.co.jp (Y. Isobe).

0022-3115/$ - see front matter © 2009 Elsevier B.V. All rights reserved.
doi:10.1016/j.jnucmat.2008.12.255

Table 1
Chemical composition of Fe–18Cr–9Ni steels.

C	Mn	Si	P	S	Ni	Cr	Cu	Fe
Composition, weight %								
Pipe measurements prior to irradiation (certificate data)								
0.09	1.36	0.38	0.025	0.020	8.75	17.66	0.21	Balance
Specification of Fe–18Cr–9Ni (X18H9, Russia)								
0.13–0.21	<2.0	<0.8	<0.03	<0.02	8.0–10.0	17.0–19.0	<0.2	Balance
AISI 304L (Japan, USA)								
<0.03	<2.0	<1.0	<0.04	<0.03	8.0–13.0	18.0–20.0	–	Balance

Table 2
Irradiation characteristics of examined specimens.

Specimen section #	Damage (dpa)	Temperature (°C)	Displacement rate (dpa/s)
1	1.7 ± 0.2	372 ± 1	$(3.8 \pm 0.4) \times 10^{-9}$
2	9.9 ± 0.3	373 ± 1	$(2.10 \pm 0.04) \times 10^{-8}$
3	12.4 ± 0.3	375 ± 1	$(2.60 \pm 0.06) \times 10^{-8}$
4	16.2 ± 0.3	373 ± 1	$(3.40 \pm 0.06) \times 10^{-8}$
5	20.5 ± 0.4	376 ± 1	$(4.30 \pm 0.08) \times 10^{-8}$

Note that all differences in dose arise only from differences in dpa rate as all specimens were derived from a single component in this constant time experiment.

Specimens were prepared from each section to study the microstructure by transmission electron microscopy. In particular, characteristics of porosity and second phase precipitates were determined. Radiation-induced changes of electrical resistivity were measured using the electrical potential technique. The measurement uncertainty in both cases was within ±0.5%.

3. Results

Microscopy revealed voids in all irradiated specimens. In Table 3 the average sizes and concentrations of the voids as well as the swelling values estimated from histograms of the void size distribution are presented. It is seen that the concentration of voids in specimens irradiated to different dpa levels have relatively similar values with the void mean radius increasing monotonically with dpa. The voids in specimens irradiated to 1.7 dpa are small, and in general they are free-standing and not associated with precipitates which exist at rather low density, but are often associated with dislocations (Fig. 1(b)). As the damage dose increases the fraction of voids associated with second phase precipitates increases and the precipitate density also increases. Void-precipitate associations at 20.5 dpa are shown in Fig. 1(h). Microdiffraction data identified the precipitates as G-phase although its lattice parameter is slightly smaller than that of classical G-phase. This phase is not normally observed at this temperature in irradiations conducted at higher dpa rate.

Other phases formed primarily along grain boundaries were identified as the M_6C and $M_{23}C_6$ carbides. In addition, extended areas of α-phase were sometimes observed to form in the γ matrix as seen at 20.5 dpa in Fig. 1(g).

Table 3
Average characteristics of voids in specimens irradiated to different dpa levels.

Section #	Damage (dpa)	Average size of voids (nm)	Concentration of voids (10^{21} m^{-3})	Swelling (%)
1	1.7	10	4.1	0.25
2	9.9	13	5.2	1.00
3	12.4	14	5.0	0.95
4	16.2	17	4.1	1.60
5	20.5	19	5.8	2.30

The electrical resistivity data of these specimens are listed in Table 4 along with the local values of swelling determined by microscopy. Since no archive pipe was available the value of 72.9×10^{-8} ohm m at 0 dpa was determined by measuring specimens from a plate produced by the same composition and melting method. This introduces the largest potential source of error in the experiment.

4. Discussion

With swelling there arise concurrent changes in electrical and elastic properties. It was shown in [1,2] that if there are no other structural changes or especially when swelling dominates the microstructure, swelling-induced changes in electrical resistance can be successfully calculated from the formula below;

$$\frac{\Delta R}{R_0} = \frac{5 \cdot S}{4 \cdot S + 6}, \quad (1)$$

where ΔR is the absolute change in electrical resistivity; R_0 is the value of the initial condition of the material, and S is the swelling represented as a volume fraction. A comparison of the measured relative change in resistivity (plotted points) to change predicted using swelling (dashed line) is shown in Fig. 2.

It is obvious that the experimental values do not follow the predicted curve, with the resistivity initially rising above the predicted curve and then falling under the curve before returning to the swelling-dominated prediction at the highest swelling level. This result shows that precipitate evolution and its concurrent effect on matrix composition is initially overwhelming the void contribution. First, if the 0 dpa value is accepted even though it is not explicitly an archive value, there appears that there may be two phase states in the evolution, one which initially increases the resistivity and a later one that decreases it. Even if the 0 dpa value is not completely representative

5. Discussion

It is often assumed that significant precipitation is not a feature of the radiation-induced microstructure of AISI 304 at temperatures and dose rates relevant to light water reactors or fast reactors in far-from-core locations. However, as shown in Fig. 3 high densities of small precipitates have been observed in AISI 304 stainless steel in EBR-II fast reactor at a near-identical temperature of 379 °C compared to the BN-600 pipe when irradiated for several decades in the lower-flux reflector regions of EBR-II [3,4]. In this case, however, the precipitates were identified as being $M_{23}C_6$ [3]. Such prolific precipitation has not been reported in this steel when irradiated at higher dpa rates in the EBR-II core. Ferrite was specifically sought but not found in 304 specimens.

The microstructural evolution observed in the present study as well as in the EBR-II case indicates that irradiation at low dpa rates for many years leads to a different precipitate microstructure and therefore different associated changes in matrix composition than are generated at higher dpa rates. Rather then to invoke only the longer times required for diffusion at lower temperatures, one possibility is that the small precipitate sizes characteristic of lower temperature irradiation are more stable at lower dpa rates, since the thermodynamic driving forces favoring precipitation must compete with the radiation-induced recoil dissolution, the latter strongest at smaller precipitate sizes and higher dpa rates.

The difference between formation of $M_{23}C_6$ and G-phase in these two examples may reflect not only small differences in steel composition, but also the somewhat higher dpa rate in the EBR-II case (1.8×10^{-7} dpa/s) vs. that of the current study

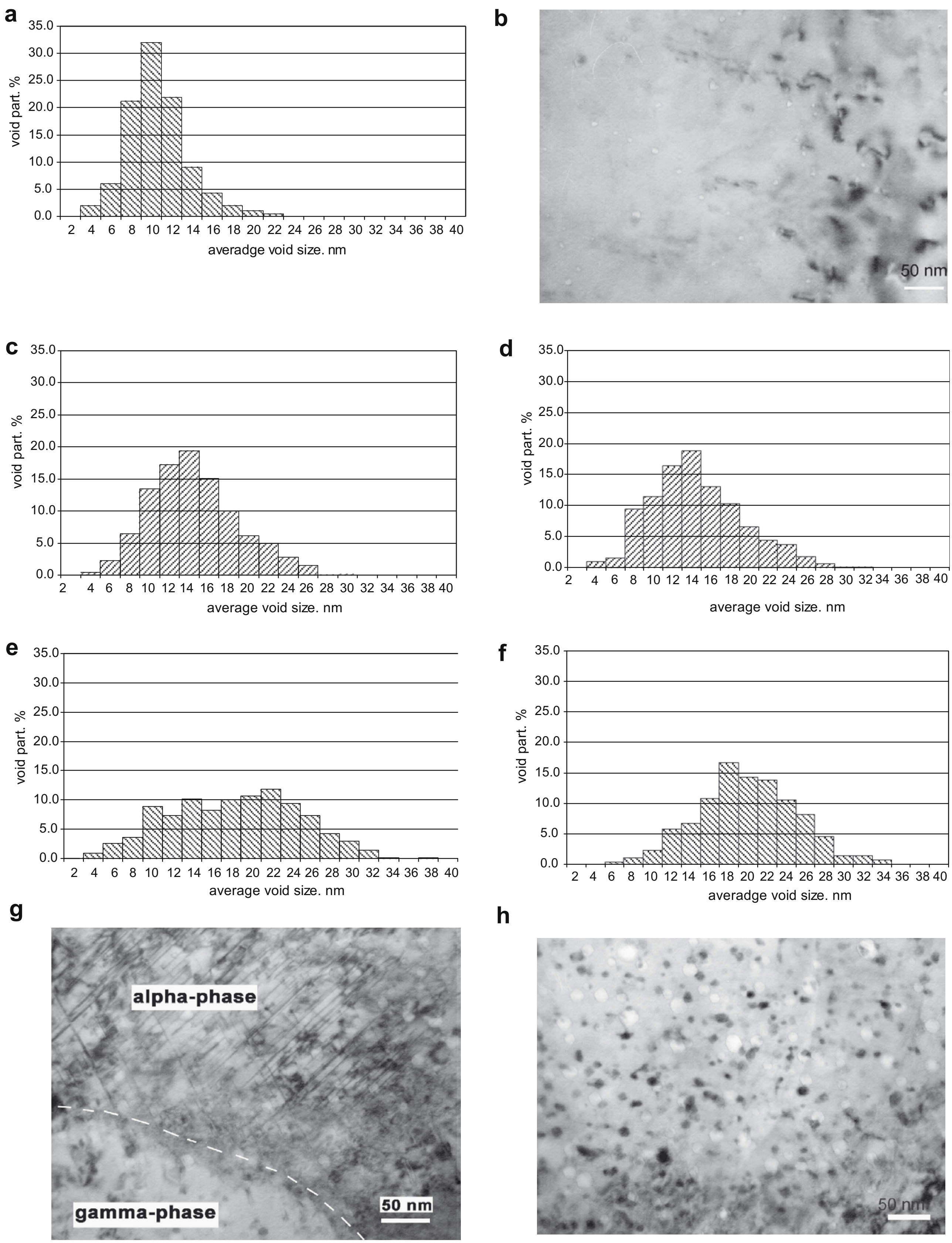

Fig. 1. Microstructures of Fe–18Cr–9Ni specimens. Panels a, c, d, e, f show histograms of void size distribution at doses of 1.7, 9.9, 12.4, 16.2 and 20.5 dpa. Voids at 1.7 and 20.5 dpa are shown in panels b and h. Occasional α-phase formation in the γ matrix is shown in panel g. Micrographs were provided in advance of publication by E. N. Shcherbakov of the Institute of Nuclear Materials.

Table 4
Average values of electrical resistivity (ρ).

Section #	Damage (dpa)	Swelling (%)	ρ (10^{-8} ohm m)
1	1.7	0.25	74.1
2	9.9	1.00	72.3
3	12.4	0.95	72.9
4	16.2	1.60	72.2
5	20.5	2.30	73.8

($\leqslant 4.3 \times 10^{-8}$ dpa/s). Borodin and co-workers have shown that radiation-induced segregation of nickel to previously formed precipitates can induce MX or carbide precipitates to change both composition and crystal structure to form G-phase [5]. Normally, G-phase formation is favored by higher nickel level or by the presence of titanium, neither of which applies to the BN-600 pipe. However, G-phase formation has been observed in Ti-free AISI 316 steel which has higher nickel content than AISI 304. [6].

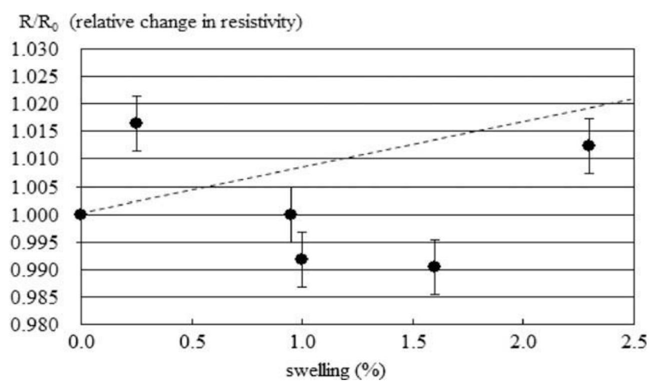

Fig. 2. Comparison of experimentally obtained relative change in resistivity (plotted points) to change predicted using swelling (dashed line).

Regardless of the phase formed, however, there will be consequences on the electrical and thermal resistivity as well as the elastic properties of the alloy matrix. Removal of carbon especially into precipitates is known to increase the density of the steel [7,8] and to change the resistivity and elasticity parameters [1,2], with the net effect depending on what other elements are removed to form the precipitate. The time-dependent phase evolution of stainless steels during irradiation is known to be exceptionally sensitive to dpa, dpa rate, temperature, irradiation history, starting thermal–mechanical treatment and both minor and major elemental compositional differences [8–11]. In some cases the austenite matrix can be transformed into ferrite by removal of nickel and other elements into precipitates [12–14].

In addition to changes arising from the compositional alteration of the alloy matrix, there may be contributions to resistivity changes arising from the crystalline state of the precipitates. Noting that α-phase was observed in the BN-600 pipe, lets consider the potential influence of forming this phase which has less electrical resistance than γ-phase and therefore should contribute to a decrease in resistance. The specific electrical resistivity of a two-phase system (a system of a single-phase matrix with unconnected second phase particle) is determined by an equation described in [15].

$$\gamma = \gamma_0 \cdot \left(1 + \frac{c}{(1-c)/3 + \gamma_0/(\gamma - \gamma_0)}\right), \tag{2}$$

where γ is the specific conductivity of the alloy; γ_0 is the specific conductivity of the matrix, γ_1 is the specific conductivity of second phase particles and c their concentration. This equation can be manipulated to yield

$$\frac{\Delta r}{r_0} = -\frac{c}{(1+2c)/3 + r_1/(r_0 - r_1)}, \tag{3}$$

where r_0, r_1 are the specific resistance of matrix and α-phase; Δr is the difference between steel containing α-phase, and without it. If $r_1 = \beta \cdot r_0$ then

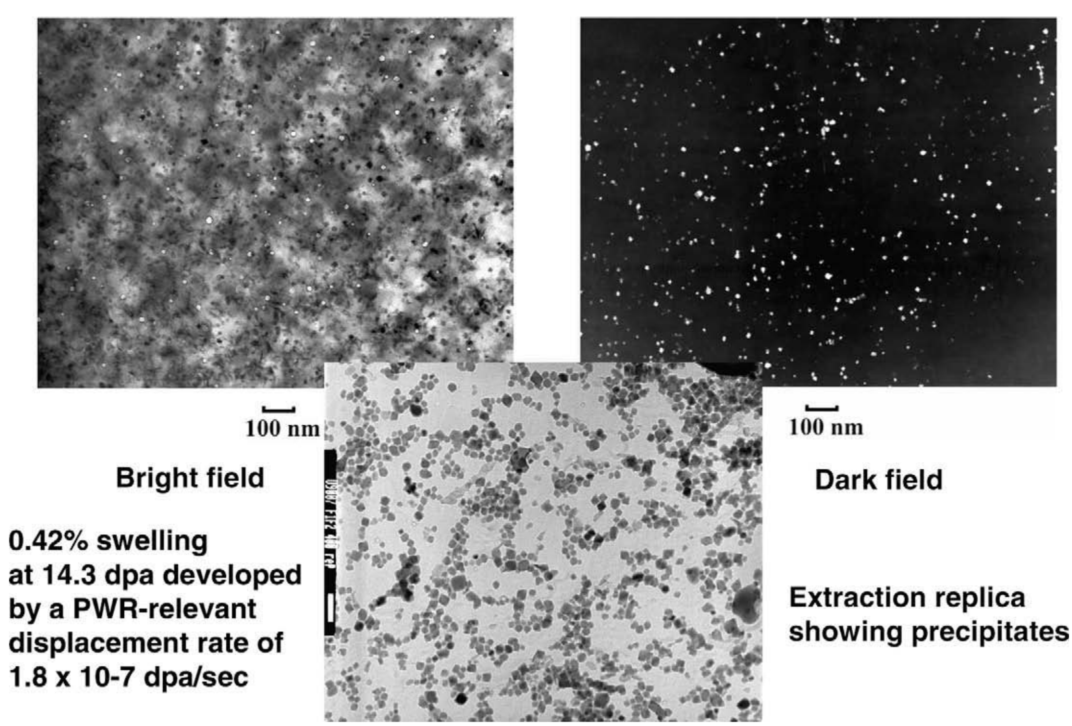

Fig. 3. Concurrent void formation and $M_{23}C_6$ precipitation after irradiation at a PWR-relevant dpa rate of 1.8×10^{-7} dpa/s in EBR-II at 379 °C, as observed in bright field, dark field and via extraction [3,4].

$$\frac{\Delta r}{r_0} = -\frac{c}{(1+2c)/3+\beta/(1-\beta)}. \tag{4}$$

Since X18H9 (Fe-18Cr-9Ni) has r_0 = 72.7 × 10^{-8} ohm m in its initial state and ferrite has r_1 = 56.6 × 10^{-8} ohm m, then β = 0, 779 and (4) transforms to

$$\frac{\Delta r}{r_0} = -\frac{c}{(1+2c)/3+3.52}. \tag{5}$$

When c is small a first approximation yields

$$\frac{\Delta r}{r_0} = -\frac{c}{3.85}. \tag{6}$$

Combining (1) and (6) yields

$$\frac{\Delta R}{R_0} = \frac{5S}{4S+6} - \frac{c}{3.85}, \tag{7}$$

and predicts that negative resistivity changes on the order of the swelling can occur for swelling levels in the 1–2% range. This suggests that it may be possible to identify the content of precipitates nondestructively using information known about the resistivity of various precipitates.

While the irradiation temperatures of the BN-600 and EBR-II cases presented in this paper are not very low compared to that in other published studies, it is significant to note that voids were observed at only 1.7 dpa at the lowest dpa rate in BN-600. This observation is consistent with a growing body of evidence that the incubation regime of void formation in austenitic stainless steels decreases progressively as the dpa rate declines, leading not only to more swelling at lower dpa rates but also to an extension of the swelling regime to lower temperatures [16–23]. Voids have been observed in several steels at very low doses at temperatures down to ~280 °C which is the inlet temperatures of the BOR-60 and BN-350 fast reactors.

6. Conclusions

The neutron-induced microstructural evolution in response to long term irradiation at 372–376 °C at very low dose rates in BN-600 was studied for a Russian low-nickel austenitic stainless steel that is analogous to AISI 304. Microstructural observation showed that in addition to voids and dislocations, an unexpectedly high density of small G-phase precipitates was formed that are not usually observed at higher dpa rates in this temperature range. A similar behavior was observed in a Western stainless steel, namely AISI 304 stainless steel, irradiated at similar temperatures and somewhat higher dpa rates in the EBR-II fast reactor, indicating that irradiation at low dpa rates for many years can lead to a different precipitate microstructure and therefore different associated changes in matrix composition than are generated at higher dpa rates. At relatively low swelling levels precipitation can cause significant deviations in resistivity compared to that predicted on the basis of void swelling alone.

Acknowledgements

This report presents a small fraction of the results of a joint study conducted at the Institute of Nuclear Materials in Zarechney, Russian Federation under Project # RUP2-1670-SK-06 funded by the Japanese Ministry of Education, Culture, Sports, Science and Technology. The contributions of Drs A. Kozlov and E. Shcherbakov to this paper are especially appreciated.

References

[1] A.V. Kozlov, E.N. Shcherbakov, S.A. Averin, F.A. Garner, in: Effects of Radiation on Materials: 21st International Symposium. ASTM STP 1447, 2003, p. 66.
[2] I.I. Balachov, E.N. Shcherbakov, A.V. Kozlov, I.A. Portnykh, F.A. Garner, J. Nucl. Mater. 329–333 (2004) 617.
[3] G.M. Bond, B.H. Sencer, F.A. Garner, M.L. Hamilton, T.R. Allen, D.L. Porter, in: F.P. Ford, S.M. Bruemmer, G.S. Was (Eds.), Ninth International Symposium on Environmental Degradation in Nuclear Power Systems – Water Reactors, The Minerals, Metals and Materials Society (TMS), 1999, p. 1045.
[4] F.A. Garner, L.R. Greenwood, in: 11th Int. Conf. on Environmental Degradation of Materials in Nuclear Power Systems – Water Reactors, 2003, p. 887.
[5] O.V. Borodin, V.N. Bryk, V.N. Voyevodin, I.M. Neklyudov, V.K. Shamardin, V.S. Neustroev, in: Effects of Radiation on Materials: 17th International Symposium, ASTM STP 1270, 1996, p. 817.
[6] P.J. Maziasz, J. Nucl. Mater. 169 (1989) 95.
[7] F.A. Garner, W.V. Cummings, J.F. Bates, E.R. Gilbert, Hanford Engineering Development Laboratory, HEDL-TME-78-9, June 1978.
[8] F.A. Garner, Materials Science and Technology: A Comprehensive Treatment, vol. 10A, VCH Publishers, 1994. p. 419.
[9] T.M. Williams, in: Effects of Radiation on Materials, 11th Conference, ASTM STP 782, 1982, p. 166.
[10] W.J.S. Yang, in: Radiation-Induced Changes in Microstructure: 13th International Symposium, ASTM STP 955, 1987, p. 628.
[11] P.J. Maziasz, J. Nucl. Mater. 205 (1993) 118.
[12] D.L. Porter, F.A. Garner, G.M. Bond, in: Effects of Radiation on Materials: 19th International Symposium, ASTM STP 1366, 2000, p. 884.
[13] H.R. Brager, F.A. Garner, in: Proceedings of AIME Symposium on Irradiation Phase Stability, Pittsburgh, PA, 5–9 October 1980, p. 219.
[14] T.M. Williams, R.M. Boothby, J.M. Titchmarsh, in: Proceedings of Materials for Nuclear Core Applications, vol. 1, Bristol, England, 27–29 October 1987, p. 293.
[15] B.G. Lifshits, V.C. Karposhin, Ya.L. Linetsky, Metallurgy (1980).
[16] T. Okita, N. Sekimura, T. Sato, F.A. Garner, L.R. Greenwood, J. Nucl. Mater. 307–311 (2002) 322.
[17] T. Okita, N. Sekimura, F.A. Garner, L.R. Greenwood, W.G. Wolfer, Y. Isobe, in: 10th International Conference on Environmental Degradation of Materials in Nuclear Power Systems – Water Reactors, 2001, issued on CD format, no page numbers.
[18] F.A. Garner, S.I. Porollo, A.N. Vorobjev, Yu.V. Konobeev, A.M. Dvoriashin, in: 9th International Conference on Environmental Degradation of Materials in Nuclear Power Systems – Water Reactors, 1999, p. 1051.
[19] S.I. Porollo, Yu.V. Konobeev, A.M. Dvoraishin, V.M. Krigan, F.A. Garner, in: 10th International Conference on Environmental Degradation of Materials in Nuclear Power Systems – Water Reactors, 2001, issued on CD format, no page numbers.
[20] S.I. Porollo, Yu V. Konobeev, A.M. Dvoriashin, A.N. Vorobjev, V.M. Krigan, F.A. Garner, J. Nucl. Mater. 307–311 (2002) 339.
[21] F.A. Garner, N.I. Budylkin, Yu.V. Konobeev, S.I. Porollo, V.S. Neustroev, V.K. Shamardin, A.V. Kozlov, in: 11th International Conference on Environmental Degradation of Materials in Nuclear Power Systems – Water Reactors, 2003, p. 647.
[22] O.P. Maksimkin, K.V. Tsai, L.G. Turubarova, T. Doronina, F.A. Garner, J. Nucl. Mater. 329–333 (2004) 625.
[23] O.P. Maksimkin, K.V. Tsai, L.G. Turubarova, T.A. Doronina, F.A. Garner, J. Nucl. Mater. 367–370 (2007) 990.